ATLAS Tile Calorimeter Time Calibration, Monitoring and Performance

ICHEP 2024, 18-24 July 2024, Prague, Czechia

Martin Divíšek (IPNP, Charles University) on behalf of the ATLAS Tile Calorimeter System

References

[1] ATLAS Collaboration. Operation and performance of the ATLAS Tile Calorimeter in Run 1. *The European Physical Journal C, 78(12), Nov 2018.*

[2] ATLAS Collaboration. Operation and performance of the ATLAS tile calorimeter in LHC Run 2. *CERN-EP-2023-266, arXiv: 2401.16034*

[3] Tile Calorimeter public plots. *https://twiki.cern.ch/twiki/bin/view/AtlasPublic/TileCaloPublicResults*.

Tile Calorimeter

- Hadronic Calorimeter used for particle energy reconstruction in the ATLAS experiment at LHC, CERN
- Passive layer made out of steel, active layer consists of scintillator 'tiles' (Fig. 1)
- Calorimeter segmented into two Long Barrel (LB) and two Extended Barrel (EB) partitions. Each partition divided into 64 modules along the azimuthal angle
- Scintillated light collected using wavelength-shifting optical fibers, converted into electric signal via photomultiplier tubes (PMTs). Tiles are grouped into cells, arranged into 3 radial layers (A, BC/B, D) and projectively in pseudorapidity (Fig. 2). Regular cells are read out by 2 PMTs (channels)
- Electric signal split into high and low gain, shaped in front-end electronics, digitized using a 10-bit ADC. Small signals amplified for better signal-to-noise ratio
- Signal amplitude, phase reconstructed in back-end via the Optimal Filtering (OF) algorithm

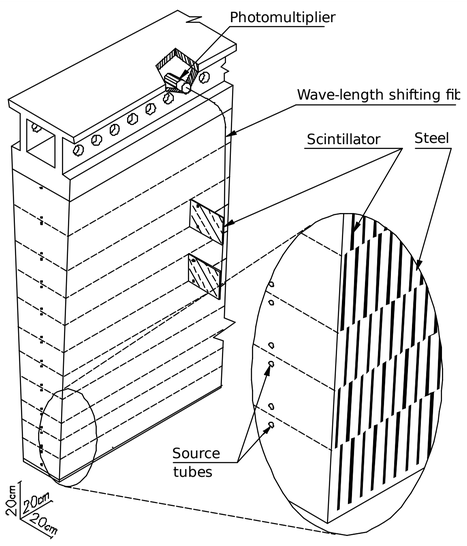

Fig. 1: TileCal Module [1]

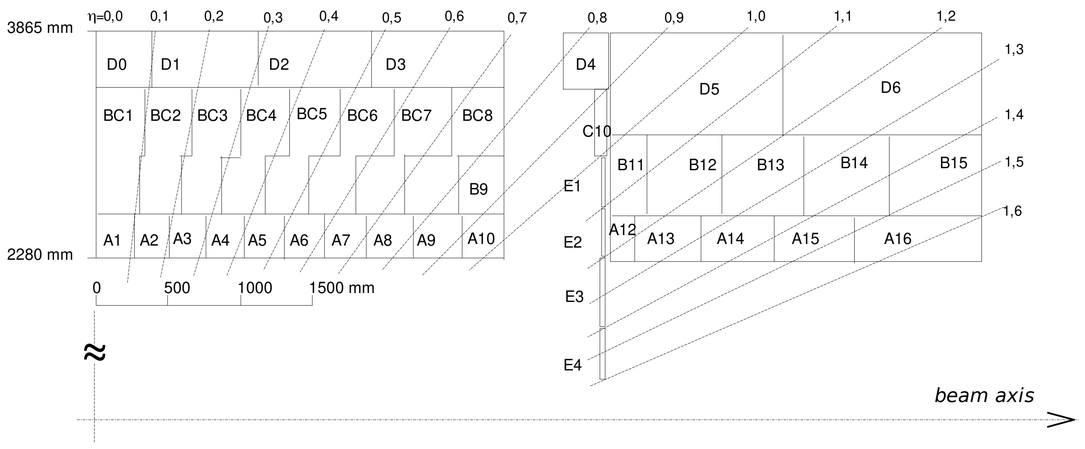

Fig. 2: Arrangement of cells in the Long and Extended Barrel [2]

Timing Jump Corrections

- Timing jumps: sudden discontinuities in cell timing caused by clock command failure at level of front-end electronics, specifically correlated across a group of six channels
- 2D histograms created for each channel using laser data (Fig. 4); reconstructed time of laser injection signal plotted vs luminosity block (lumiblock – time interval of data recording)
- Automatic software tool uses a floating average to scan for anomalies in mean reconstructed time on a per-channel basis
- Timing Jump detection threshold recently lowered from 3 ns down to 1 ns thanks to upgrade of the software tool
  - Floating average method kept, method for timing data storage rebuilt from scratch – now handled via custom dedicated class
  - Full backward compatibility with older data, minimal increase in memory and storage space reqs., multiple additional checks introduced
  - Applied during 2022 and 2023 reprocessing, over 70% of all detected jumps below original 3 ns detection threshold in both years

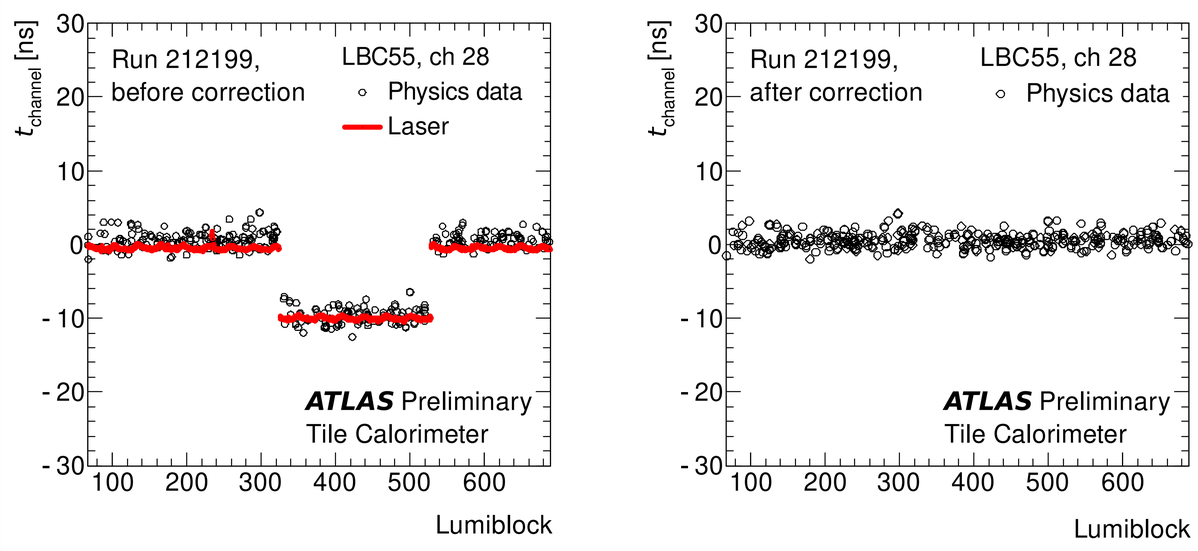

Fig. 4: Example timing jump, before and after corrections [1]

Time Calibration and Monitoring

- Precise TileCal energy reconstruction requires time calibration for optimal performance (OF algorithm is phase-dependent, correct particle time-of-flight necessary)
- Individual channels must be calibrated to yield zero-phase signal in response to ultra-relativistic particles travelling from the detector interaction point
- Time calibration and monitoring achieved using *pp* jet data, muon splashes
- Time monitoring also utilizes data from laser calibration system; illumination of all PMTs by controlled light source, either in-gap during empty bunch crossings of a *pp* run or during dedicated standalone runs
- Zero phase fixed via introduction of channel-specific time constants reflecting e.g. length of optical fibers, time-of-flight into the specific cell, ...
- Corrections to channel timing performed during calibration loop for each run as well as during yearly reprocessing (Fig. 3)
- Software tools allow bulk analysis and monitoring of channel timing during the run

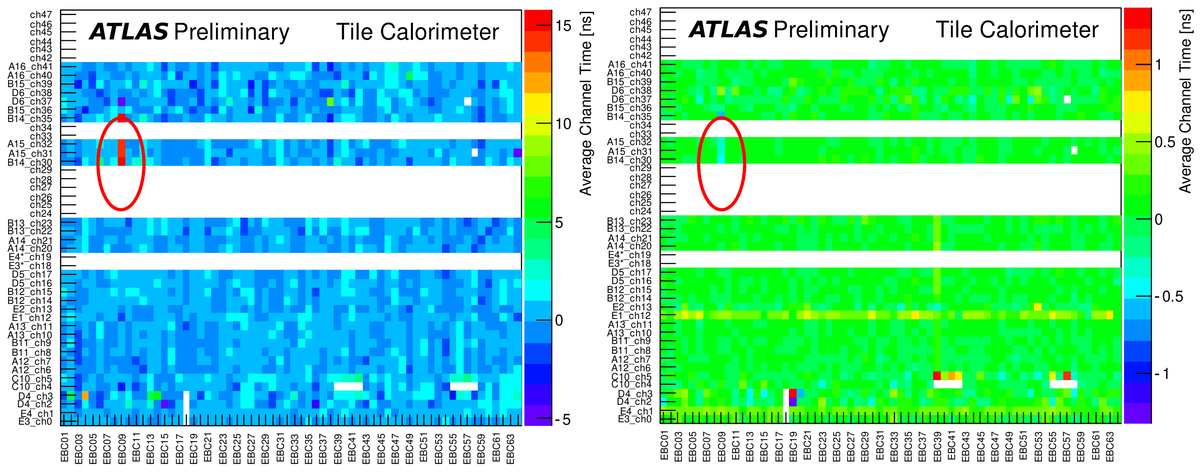

Fig. 3: Mean channel times in physics, before and after corrections [3]

Time Resolution

- Gaussian fit applied to the distribution of reconstructed times in a specific cell energy range – time resolution denotes the width of the fitted gaussian
- Dependence of detector time resolution on energy routinely monitored and investigated
  - Detector time resolution fitted by the formula listed in Fig. 5 in both gains separately
  - Formula divided into three terms summed in quadrature, based on correspondence to the OF algorithm weights
- Detector time resolution can now be examined in each individual radial layer (previously only analysis at the level of individual partitions available)
- Qualitative explanation of observed effects based on detector geometry and impacts of pile-up for specific cell types available:
  - Relative differences between Long and Extended Barrels for each individual radial layer caused by differences in absolute pseudorapidity of cell centers – resolution worsens with increased pseudorapidity
  - Outermost D-layer time resolution offset at higher energies caused by greater cell size in the pseudorapidity frame – resolution worsens with cell size (see Fig. 2)
  - Innermost A-layer low energy behaviour driven by pile-up sensitivity – time resolution degrades with increased pile-up

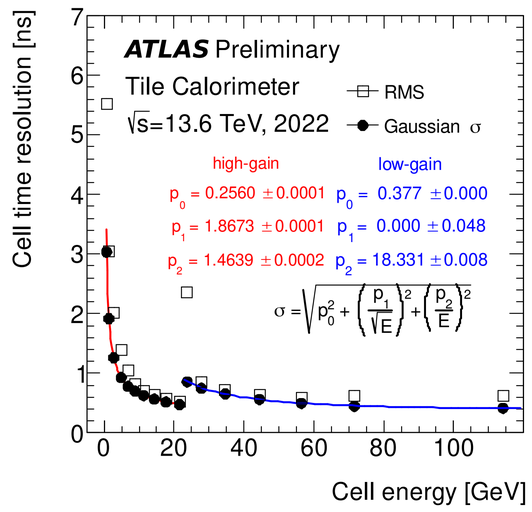

Fig. 5: Combined Time Resolution [3]

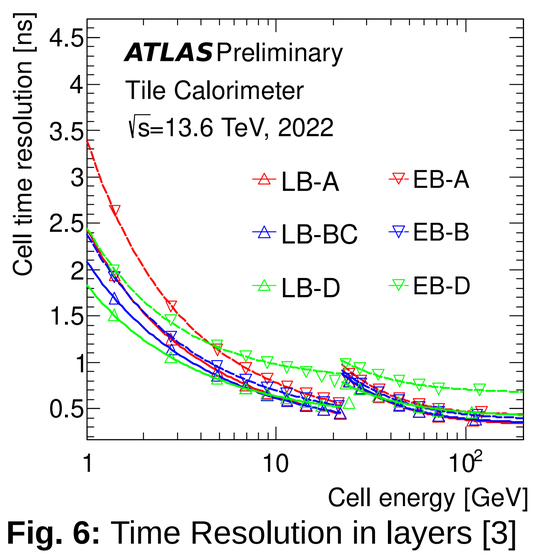

Fig. 6: Time Resolution in layers [3]